γ and β cerium: LDA+U calculations of ground-state parameters

B. Amadon, F. Jollet, and M. Torrent
Département de Physique Théorique et Appliquée, CEA, Bruyères-le-Châtel, 91297 Arpajon Cedex, France
(Received 4 June 2007; revised manuscript received 30 October 2007; published 2 April 2008)

In this paper, we present a study of the β phase of cerium. We show that this is a correlated phase like γ cerium. Their structural parameters and the antiferromagnetic ground state of β Cerium are correctly described within the local density approximation with a Hubbard parameter U (LDA+U). We also discuss the problem of the search for the ground state of the system. The calculations are done within the projector augmented wave framework.

DOI: 10.1103/PhysRevB.77.155104 PACS number(s): 71.20.Eh, 71.27.+a, 71.15.Ap, 71.15.Mb

I. INTRODUCTION

Cerium is the first of the rare earth metals. It has been experimentally and theoretically studied especially to understand the mechanism of the volume collapse of the isostructural α-γ transition.[1] In the low pressure and low temperature domain, it exhibits three phases[1] (see Fig. 1): The low temperature α and high temperature γ phases have a fcc structure, whereas the β phase is double hcp (dhcp).

The magnetic properties are different: The α phase has a Pauli paramagnetism. The γ and β phases have a local moment that is antiferromagnetically ordered in the β phase, whereas the γ phase has a Curie–Weiss susceptibility. The existence of a local moment suggests that the f electrons are localized, at least in γ and β. This comes from the very localized $4f$ orbitals, which induce strong correlations between electrons.[2] Let us note, however, that the difference between α and γ phases only reflects the difference in magnitude of the hybridization and, thus, of the Kondo temperature. Below the Kondo temperature of both phases, we expect the two phases to be similar: In this case, the existence of the transition is under discussion.[3] If electronic structure calculations using density functional theory (DFT) in the local density approximation (LDA)[4,5] correctly describe the ground-state properties of a lot of insulators, semiconductors, and simple metals, they usually fail for correlated systems containing open $3d$, $4f$, or $5f$ shells. For example, DFT calculations within either LDA or generalized gradient approximation (GGA) exchange and correlation functionals fail to describe the γ phase of cerium (the lattice parameter is underestimated by 12% in LDA): An explicit description of electronic interactions is thus necessary. Since the beginning of the 1990s, new methods have been explicitly designed to describe these particular cases. Some of these methods contain an explicit description of the strong electronic correlation in the subset of correlated orbitals. Namely, the local density functional with a Hubbard parameter (LDA+U) method[6–9] has been able to describe oxides of transition metals, rare earths, and actinides, in which the local correlations are strong. More recently, LDA+U has been used to describe correlated metals.[10–12] It appears that this method gives a good description of these systems at the expense of creating an artificial magnetic order—except in some special cases.[13] The LDA+DMFT [14–17] method, which is a combination of LDA and dynamical mean field theory (DMFT), is a more general formalism and can correct this deficiency. It has been successfully used to describe systems, such as cerium α and γ phases, in which electrons are between localization and delocalization.[18–24] As LDA+U is only a static version of LDA+DMFT, it might be unable to describe weakly correlated phases. We also expect that, even in this case, the bandwidth of high energy bands will not be correct. A recent work[25] on magnetically ordered models showed that a static mean field is valid only for the ground-state parameters, with respect to DMFT. It showed that LDA+U should be used only to compute ground-state properties. Finally, note that self-interaction correction schemes have also been designed in order to describe cerium.[26,27]

Some LDA+U calculations have been carried out to describe localized phases in rare earths. In gadolinium,[28–30] the method yields correct structural parameters for the hcp phase. Moreover, this phase is ferromagnetic (FM). Calculations such as LDA calculations, where the f states are located at the Fermi energy, show that the antiferromagnetic (AFM) order is more stable. Contrarily, LDA+U or calculations using frozen f electrons reproduce the correct magnetic order.[28–30] This is attributed to the incorrect interaction of f states with other orbitals when they are located at the Fermi level.

To our knowledge, only a few theoretical studies have been devoted to β cerium.[31,32] These studies intended to compute the band structure and density of states either by a Korringa-Kohn-Rostoker (KKR) approach[31] with an exchange term or by DFT within the GGA exchange correla-

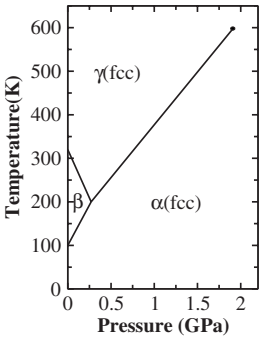

FIG. 1. Phase diagram (Ref. 1) of cerium in the low temperature and low pressure domain. The α and γ phases have a fcc structure. The β phase has a dhcp structure.

tion potential.[32] However, due to the similarity between the structural parameters of β and γ cerium and also to the existence of a local moment in both phases, it is expected that the two phases should both be described within a scheme that takes into account strong correlations. In this paper, we show that LDA+U is able to describe both γ and β cerium phases. Similar to hcp gadolinium, we find that this method correctly describes the energetic order between the antiferromagnetic and ferromagnetic solutions for β cerium.

In the first part of this paper, we review some aspects of the LDA+U formalism that are useful for this work. We give some details on our implementation of LDA+U within the projector augmented wave (PAW) code ABINIT (Refs. 33–35) (with some refinements for the calculation of the occupation matrix). We then check that standard results are reproduced within our implementation. The second and main part is devoted to calculations on γ and β phases of cerium.

II. LDA+U METHOD IN THE PROJECTOR AUGMENTED WAVE METHOD

In this section, we briefly review the LDA+U framework and its implementation within PAW, and we show some tests of our implementation.

A. LDA+U method

The LDA+U method[6–9] has been designed from the combination of density functional theory and a Hubbard-type term in the Hamiltonian. The contribution to energy is the sum of the LDA energy for a given density, the electron-electron interaction term E_{ee} from the Hubbard term, and a double counting term $(-E_{dc}):E_{LDA+U}[n_{LDA+U}]=E_{LDA}[n_{LDA+U}]+E_{ee}-E_{dc}$. The last two terms are functions of the occupation matrix $n^{\sigma}_{1,2}$ in a given basis.

In the rotationally invariant form, E_{ee} is[8]

$$E_{ee}=\frac{1}{2}\sum_{1,2,3,4}\sum_{\sigma}[\langle 13|24\rangle n^{\sigma}_{1,2}n^{-\sigma}_{3,4} + (\langle 13|24\rangle-\langle 13|42\rangle)n^{\sigma}_{1,2}n^{\sigma}_{3,4},], \quad (1)$$

where σ stands for the spin. Atom indices are neglected for clarity. $\langle 13|24\rangle$ are matrix elements of the interaction V_{ee} and are related to Slater integrals F_k (Refs. 7 and 36) and Gaunt coefficients $\langle m_1|m|m_2\rangle$, thanks to

$$\langle 13|24\rangle=\langle m_1,m_3|V_{ee}|m_2,m_4\rangle = 4\pi\sum_{k=0,2,4,6}\frac{F_k}{2k+1}\sum_{m=-k}^{+k}\langle m_1|m|m_2\rangle\langle m_3|m|m_4\rangle, \quad (2)$$

where m, m_1, and m_2 stand for real spherical harmonics. The double counting term is supposed to cancel the local electron-electron interaction already described in LDA. In the full localized limit (FLL), it corresponds to the value of E_{ee} in a reference system in which the occupation matrix is diagonal and diagonal elements are whole numbers. The corresponding expression is[6,8,9]

$$E^{FLL}_{dc}=U\frac{1}{2}N(N-1)-J\sum_{\sigma}\frac{1}{2}N^{\sigma}(N^{\sigma}-1). \quad (3)$$

In contrast, the "around mean field" (AMF) version is designed to correct a system in which electrons are equally shared among correlated orbitals. E^{AMF}_{dc} is then[9]

$$E^{AMF}_{dc}=UN_{\uparrow}N_{\downarrow}+\frac{1}{2}(N^2_{\uparrow}+N^2_{\downarrow})\frac{2l}{2l+1}(U-J). \quad (4)$$

From these expressions of energy, the derivation of the potential on the basis of correlated orbitals can be done.[8] We obtain $V^{FLL}_{dc,\uparrow}=U(N_{\downarrow}+N_{\uparrow}-1/2)-J(N_{\uparrow}-1/2)$ and $V^{AMF}_{dc,\uparrow}=UN_{\downarrow}+(U-J)N_{\uparrow}\frac{2l/2l+1}{}$ for the double counting part.

Note that the LDA+U rotationally invariant form proposed by Dudarev *et al.*[37] is equivalent to the FLL version of LDA+U with $J=0$ and with U in place of $\bar{U}-\bar{J}$: $E_{ee}-E_{dc}=\frac{\bar{U}-\bar{J}}{2}\Sigma_{\sigma}[\mathrm{Tr}(n^{\sigma})-\mathrm{Tr}(n^{\sigma}n^{\sigma})]$, where $\bar{U}-\bar{J}$ are the spherically averaged value of U and J.[37]

In the present paper, we use these three schemes and carefully compare the corresponding results.

B. Projector augmented wave implementation

The projector augmented wave method,[38] which is associated with plane waves, is particularly adapted to the description of complex phases in which atomic relaxations are important. Another advantage of PAW is that the nodal structure of the wave function is correct. Moreover, the frozen core approximation can be controlled through the inclusion of more and more states in the valence band.

TABLE I. Gap in eV and magnetic moment for NiO compared to other LDA and LDA+U calculations and to the experiment. η: $U=8.0$ eV and $J=0.0$ eV; elsewhere: $U=8.0$ eV and $J=0.95$ eV.

		PAW[b]			PAW[c]	FLAPW[d]		FPLMTO[e]
	Expt.[a]	LDA	LDA+U	LDA+U$^{\eta}$	LDA+U$^{\eta}$	LDA	LDA+U	LDA+U
μ_s	1.64–1.90	1.23	1.74	1.74	1.83	1.186	1.687	1.74
Gap (eV)	4.0–4.3	0.5	3.3	3.3	4.1	0.41	3.38	3.4

[a]References 42–46.
[b]This work.
[c]Reference 39.
[d]Reference 12.
[e]Reference 47.

In the following, we adopt the original notations of Blöchl[38] for the wave functions and for atomic data sets. Our implementation of LDA+U within PAW mainly follows the line of work of Bengone *et al.*[39] The main ingredient of the LDA+U implementation is the occupation matrix $n^{\sigma}_{m,m'}$ in a given localized orbital basis (χ_m). We can write the occupation matrix as [with $P_{m,m'}=|\chi_m\rangle\langle\chi_{m'}|$ (Ref. 39)]

$$n^{\sigma}_{m,m'} = \sum_{\mathbf{k},n} f_n^{\mathbf{k},\sigma}\langle\Psi_n^{\mathbf{k},\sigma}|P_{m,m'}|\Psi_n^{\mathbf{k},\sigma}\rangle = \sum_{\mathbf{k},n} f_n^{\mathbf{k},\sigma}\langle\tilde{\Psi}_n^{\mathbf{k},\sigma}|\tilde{P}_{m,m'}|\tilde{\Psi}_n^{\mathbf{k},\sigma}\rangle, \tag{5}$$

where $f_n^{\mathbf{k},\sigma}$ and $\Psi_n^{\mathbf{k},\sigma}$ are occupation numbers and Bloch functions for a given k-point $\mathbf{k}$, band index n, and spin σ. For χ_m, we use the ground-state atomic orbital ϕ_0. We are interested in the description of systems in which correlated orbitals are localized. For these systems, we expect that the norm of χ_m computed inside a sphere will be close to 1. We have then decided to define the projector operator $P_{m,m'}$ only inside the augmentation region. The influence of this approximation can be checked by increasing the PAW matching radius. We may then use the expression for an operator A within the PAW formalism [Eq. (11) of Ref. 38]. This expression can only be used for a local operator and a nonlocal operator defined only inside the augmentation region. The first and last terms cancel inside the augmentation region if the basis is complete in the range of energy of interest, so we have to take into account only the second one, and the occupation matrix is then (with $A=P_{m,m'}$) (i is a shorthand notation for l_i,m_i,n_i: angular momentum, projection of angular momentum, and PAW projector)

$$\begin{aligned} n^{\sigma}_{m,m'} &= \sum_{\mathbf{k},n} f_n^{\mathbf{k},\sigma}\sum_{ij}\langle\tilde{\Psi}_n^{\mathbf{k},\sigma}|\tilde{p}_i\rangle\langle\phi_i|P_{m,m'}|\phi_j\rangle\langle\tilde{p}_j|\tilde{\Psi}_n^{\mathbf{k},\sigma}\rangle \\ &= \sum_{n_i,n_j,l_i=l_U}^{m_i=m,m_j=m'} \rho^{\sigma}_{ij}\langle\phi_{n_i}|\phi_0\rangle\langle\phi_0|\phi_{n_j}\rangle, \end{aligned} \tag{6}$$

where LDA+U is applied to the angular momentum l_U and

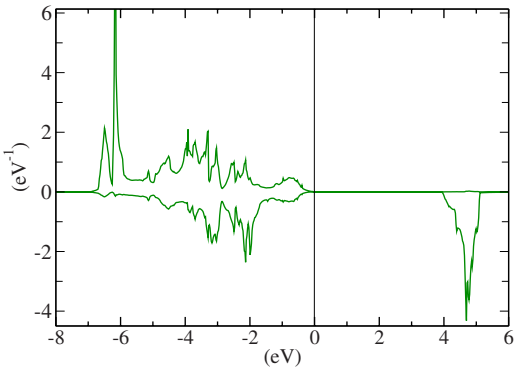

FIG. 2. (Color online) Projected d-density of states of NiO in LDA+U.

$\rho^{\sigma}_{ij}=\Sigma_{n\mathbf{k}} f_n^{\mathbf{k},\sigma}\langle\tilde{\Psi}_n^{\mathbf{k}\sigma}|\tilde{p}_j\rangle\langle\tilde{p}_i|\tilde{\Psi}_n^{\mathbf{k}\sigma}\rangle$. For $l_i=l_U$, we use the notation $\phi_{m_i,n_i}=\phi_{n_i}Y_{l_U,m_i}$. We emphasize that in Eq. (6), $\langle\phi_{n_i}|\phi_0\rangle$ and $\langle\phi_0|\phi_{n_j}\rangle$ are integrals computed inside the sphere delimited by the PAW matching radius. Note that this is in contrast to a previous study[39] in which the authors have chosen

$$n^{\sigma}_{m,m'} = \sum_{n_i,n_j} \rho^{\sigma}_{ij}\langle\phi_{n_i}|\phi_{n_j}\rangle. \tag{7}$$

However, this last scheme induces only a small variation of 0.2% with respect to our choice concerning lattice parameters in cerium (see below for details of the calculation).

From the occupation matrix, energy is directly calculated from Eq. (1). The DFT double counting expression for energy (involving the sum over Kohn–Sham eigenvalues) is also computed as a check of the coherence of the implementation.

The LDA+U Kohn–Sham potential, which is computed[39] following Blöchl,[38] is deduced from the energy with $H^{\sigma}=dE/d\rho^{\sigma}$, where $\tilde{\rho}^{\sigma}=\Sigma_{n\mathbf{k}}|\tilde{\Psi}^{\sigma}_{n\mathbf{k}}\rangle f^{\sigma}_{n\mathbf{k}}\langle\tilde{\Psi}^{\sigma}_{n\mathbf{k}}|$. For $E_U=E_{\text{e-e}}-E_{\text{dc}}$, it gives

TABLE II. Lattice parameters of Gd in the AFM and FM ground states and energy difference (in meV/atom) between the AFM and FM states (at the relaxed lattice parameters for the FM and AFM order and also for the unrelaxed case) of hcp gadolinium according to experimental data and calculations within LDA+U (U=6.7 eV and J=0.7 eV) and LDA. †: Our calculation. Values from other theoretical works (‡): are given (Refs. 28, 29, and 48). $\Delta a/a=(a_{\text{theor}}-a_{\text{expt}})/a_{\text{expt}}$. Experimentally, a=3.63 Å, c/a=1.597, and $E_{\text{AFM}}-E_{\text{FM}}>0$. Calculations by Kurz *et al.* (Ref. 29) are done at fixed c/a=1.597.

	LDA+U‡	LDA+U†	LDA‡	LDA†
$(\Delta a)/a$ (FM) (%)	−2.8 [a]	−2.8	−3.9 [a]	−4.0
c/a (FM)		1.595		1.606
$(\Delta a)/a$ (AFM) (%)	−3.5 [a]	−3.5	−4.6 [a]	−4.2
c/a (AFM)		1.610		1.588
$E_{\text{AFM}}-E_{\text{FM}}$ (relaxed)	34[a]	16	−68,[b] −69,[a] −56 [c]	−32
$E_{\text{AFM}}-E_{\text{FM}}$ (unrelaxed)	63,[d] 26–51[a]	28	−2 [d]	−7

[a]Reference 29.
[b]Reference 43.
[c]Reference 49.
[d]Reference 28.

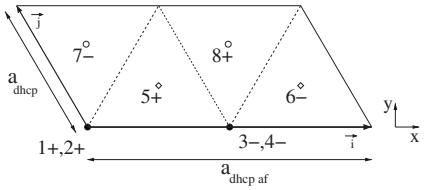

FIG. 3. View along z of the geometric structure of the unit cell of the β phase of cerium in a proposed AFM structure (Ref. 54). Only atoms in the unit cell are shown and numbered. For example, atoms 5 and 6 are first neighbors of atom 3. The sign (+ or −) is a notation for the spin. Atoms 1–4 (which belong to layer A) are in a cubic environment and atoms 5–8 (which belong to layers B and C) are in a hexagonal environment ($\diamond$: $z=1/4$; $\bigcirc$: $z=3/4$). The usual dhcp structure is one-half of this unit cell. For the antiferromagnetic structure, three parameters are necessary to define the unit cell: $a(=a_{\mathrm{dhcp}})$, $b(=a_{\mathrm{dhcpaf}})$, and c.

$$H^{\sigma}=\frac{dE_U}{d\tilde{\rho}^{\sigma}}=\sum_{i,j}^{l_i=l_j=l_U}\underbrace{\frac{dE_U}{dn^{\sigma}_{m_im_j}}}_{V^{\mathrm{LDA+U}}_{m_im_j}}\underbrace{\frac{dn^{\sigma}_{m_im_j}}{d\rho^{\sigma}_{ij}}}_{C_{n_in_j}}\underbrace{\frac{d\rho^{\sigma}_{ij}}{d\tilde{\rho}^{\sigma}}}_{|\tilde{p}_i\rangle\langle\tilde{p}_j|}=\sum_{i,j}^{l_i=l_j=l_U}|\tilde{p}_i\rangle D^U_{ij}\langle\tilde{p}_j|. \tag{8}$$

The first derivative is the LDA+U potential $V^{\mathrm{LDA+U}}$ computed[8] by the derivation of E_{ee} with respect to n_{m_i,m_j}. We then have $D^U_{ij}=V^{\mathrm{LDA+U}}_{m_im_j}C_{n_in_j}$, which is a contribution to the nonlocal part of the Hamiltonian.[40]

Note that the LDA+U energy explicitly depends on the cell parameters only through $n^{\sigma}_{m,m'}$ and, therefore, the projectors $\tilde{p}_i$. The only explicit LDA+U contribution to the forces and stress is thus contained in D_{ij} in Eq. (55) of Ref. 40 and Eq. (38) of Ref. 41. There is also an implicit contribution through the electronic density.

C. Test of the code

In order to validate our implementation, we show here some tests of our code on antiferromagnetic nickel oxide and on gadolinium.

1. Nickel oxide

LDA underestimates the gap and the magnetic moment in nickel oxide. They are better described in LDA+U.[6] In our calculation, 3s and 3p semicore states are treated in the valence for nickel. Valence states for oxygen are 2s and 2p. The PAW matching radii are 2.3 and 1.91 a.u. for nickel and oxygen, respectively. The energy cutoff for the plane wave expansion of the pseudo-wave function is 24 hartree. In this case, there is no more variation of the spin moment within less than 0.1%. The energy is converged within less than 0.5 mhartree. The lattice parameter is fixed at the experimental value (4.19 Å). 864 k points are used in the full Brillouin zone. 97.5% of the d atomic wave function is contained inside the augmentation region. The values for U and J are given in Table I. The FLL version of the double counting term is used. Our density of states projected on d orbitals is shown in Fig. 2. The LDA and LDA+U results are compared to other calculations in Table I. The spectrum shows that the physical picture is correct. The magnetic moment, which is computed by doing the difference of the integrals of up and down densities, is $1.74\mu_B$. The value of the gap obtained from our calculation is 3.3 eV. However, if we take into account the point where the conduction band becomes really important, we find a value of 4.0 eV. We see that our values for the gap and the spin moment are in the range of existing LDA+U implementations, including full linear augmented plane wave (FLAPW) calculations. The variation of the gap upon the choice of the PAW matching radius or the expression of the density matrix [Eq. (6) or (7)] is lower than 0.1eV.

TABLE III. Lattice parameter a and bulk modulus B_0 of γ cerium according to experimental data and calculations within all -electron methods in LDA.

	Expt.[a]	LDA[b]	GGA[b]	LDA[c]
a (a.u.)	9.76	8.49/8.55	8.89/8.86	8.54
a (Å)	5.16	4.49/4.52	4.70/4.69	4.52
B_0 (GPa)	19/21	60.5/58.8	48.7/42.9	59

[a]References 57 and 58.
[b]References 55 and 56.
[c]This work.

2. Gadolinium

hcp gadolinium is a ferromagnet described as an antiferromagnet in LDA. LDA+U calculations[28–30] correct this deficiency and also more correctly describe the atomic structure. In our calculations, the PAW data set is generated with a PAW matching radius of 2.4 a.u. The 5s and 5p semicore states are treated as valence states. A value of 16 hartree for the energy cutoff of the plane wave expansion is sufficient to converge the difference in energy between the ferromagnetic and antiferromagnetic solutions to the precision given in Table I. 2560 k points are used in the full Brillouin zone. The FLL double counting term is used. For the ferromagnetic and antiferromagnetic calculations, we find a magnetization per atom value of $7.6\mu_B$—which is in good agreement with the experimental value [$7.63\mu_B$ (Ref. 28)]—and $7.44\mu_B$. The difference in magnitude of the magnetic moment between the two magnetic configurations is consistent with other results.[28,29]

The structural parameters given in Table II are in good agreement with results obtained in the FLAPW calculations of Kurz *et al.*[29] The LDA results for the difference in energy between the ferromagnetic and antiferromagnetic solutions are in reasonable agreement with the results of other calculations. In LDA+U, we reproduce the previous results where the ferromagnetic solution is lower in energy. The difference in energy is 16 meV/atom, which is less than the value found by Kurz *et al.*[29] (34 meV/atom) but is in the same order of magnitude. Similar results are found for unrelaxed calculations. As mentioned by Kurz, this difference in energy depends on the radius of the sphere, in which the LDA+U correction is applied. Kurz *et al.*[28] used 2.8 a.u., while we used 2.4 a.u. Another difference comes from the wave func-

TABLE IV. Lattice parameter and bulk modulus of γ cerium according to experimental data and calculations within LDA+U (U=6.1 eV and J=0.7 eV). Calculations with f electrons in the core are also presented. $\Delta a/a=(a_{\text{theor}}-a_{\text{expt}})/a_{\text{expt}}$.

		LDA+U		LDA		
	Expt.[a]	FLL[b]	FLL[c]	fcore[d]	fcore[c]	LDA[c]
a (a.u.)	9.76	9.83	9.52	9.69	9.63	8.54
a (Å)	5.16	5.20	5.04	5.12	5.09	4.51
$\Delta a/a$ (%)	0.0	0.7	−2.4	−0.7	−1.3	−12.4
B_0 (GPa)	19	29.6	34	31	34	59

[a]References 57 and 58.
[b]Reference 12.
[c]This work.
[d]Reference 60.

tions used to compute the occupation matrix: They are not the same in our calculation and in the FLAPW implementation. However, all of these LDA+U calculations correctly reproduce the stability of the FM state.

III. RESULTS AND DISCUSSION

In this section, we first present the PAW data set used and the computational details. Then, we present our description of γ and β cerium.

A. Generation of the projector augmented wave data set

The PAW data set was generated with the code ATOMPAW.[50,51] The Vanderbilt projector generation scheme[52] is used, and the PAW matching radius is 2.45 a.u. The 5s and 5p semicore states are treated as valence electrons. Two projectors per angular momentum are used. We check the validity of the reference energies by using calculations involving three f projectors and also by inspecting the logarithmic derivatives with respect to the energy of the pseudo-wave function computed at the PAW matching radius. A value for the energy cutoff of 12 hartree is sufficient to converge the energy within 1 mhartree. We have also done some calculations at 16 hartree as a check.

B. Computational details

An important point in LDA+U calculations concerns the values of U and J. We use values computed by constrained LDA,[53] namely, U=6.1 eV and J=0.7 eV, for calculations that use the scheme of Liechtenstein *et al.*[8] For the scheme of Dudarev *et al.*,[37] we use the value $U-J$=5.4 eV. However, the results are insensitive to the precise value of U and to the LDA+U scheme used, as shown below. The k-point sampling is done by the special k-point method. For γ fcc cerium, 4000 k points in the full Brillouin zone (BZ) are sufficient to have a precision better than 1 GPa on the bulk modulus and other better than 0.5% on the volume. A small Gaussian smearing of 2.7 meV is used. For β cerium, the AFM unit cell is used [eight atoms per unit cell (see Fig. 3)] in order to make a direct comparison between the FM and AFM[54] cases. We use 728 k points in the full BZ with the same smearing. We then have nearly the same density of k points in the BZ for the two structures, and it is then sufficient to have the same precision as that for γ cerium. Moreover, the differences in energy are converged within less than 1 meV/atom, which is sufficient for our purpose.

C. Calculation on cerium

1. γ cerium

In order to test our PAW data set, we have first carried out standard LDA calculations. The results are summarized in Table III. Our results are within the range of available calculations done within the full potential linear muffin tin orbital (FP-LMTO) method.[56,57] This shows that our PAW data set is correct. We have not taken spin-orbit coupling into account because we assume that its effect is negligible.

To describe the paramagnetic γ phase, one should use a method beyond the static mean field, such as DMFT.[18,19,22,24,59] In LDA+U, we find that one has to impose a magnetic order. For simplicity, we choose a ferromag-

TABLE V. Structural parameters of γ cerium according to experimental data and calculations within LDA+U (for FLL and AMF: U=6.1 eV and J=0.7 eV; for the Dudarev scheme: U=5.4 eV).

		LDA+U			GGA+U
	Expt.[a]	FLL	AMF	Dudarev	FLL
a (a.u.)	9.76	9.52	9.43	9.54	9.95
a (Å)	5.16	5.04	4.99	5.05	5.27
B_0 (GPa)	19	34	30	33	28

[a]References 57 and 58.

netic order. Table IV shows a comparison of the structural parameters to the calculation of Shick *et al.*[12] with the same U and J parameters.

We first note that the inclusion of LDA+U increases the equilibrium volume because the electrons are localized and no longer participate in the bonding. The results are rather insensitive to the precise values of U and J. A variation of $U-J$ by ± 1 eV—which is beyond the range of reasonable values quoted in the literature[54,60]—induces a variation of ± 0.04 a.u. for the lattice parameter. The LDA+U calculation slightly underestimates the lattice parameter of cerium, as was done for the lattice parameter of gadolinium. However, we note a disagreement between our calculation and the calculation of Shick *et al.*[12] We suggest that it is a consequence of the different basis functions used in LDA+U.

Moreover, we carried out a calculation with the f states in the core. For this purpose, we created a PAW data set without any f projectors. The structural parameters in this case, which are given in Table IV, are in good agreement with the parameters used in the LMTO-Atomic sphere approximation (ASA) calculation with f electrons in the core, which was done by Johansson *et al.*[61] As expected, LDA+U gives a volume lower than that from calculations done with frozen f electrons. However, our goal is not to precisely compute the volume of the γ and β phases of cerium. Moreover, these are high temperature phases, and entropic contributions are expected to be non-negligible.[24,62]

In order to validate our method, we have carried out a few calculations with three flavors of the LDA+U method.[8,9,37] The results are presented in Table V. The FLL method and the spherically averaged one[37] give the same result.

We see that the AMF method underestimates the volume of the γ and β phases even more. We can, in fact, show that the AMF method is not fit for the LDA+U calculations on cerium: As LDA+U is a self-consistent scheme, the double counting term must correct the LDA Hamiltonian with LDA+U occupations. In particular, the AMF method is made to correct a system in which the electrons are equally distributed among orbitals. Thus, it is not suitable for cerium, where the converged solution in LDA+U contains one electron localized into one orbital. As there is only one f electron in cerium, the inclusion of the J parameter is not necessary. We will then use the spherically averaged method, which has only one parameter in the study of the β phase. Physically, the magnetic moment is logically insensitive to the choice of the method and is equal to $1.1\mu_B$ whatever the LDA+U method used. For reference, we have also included the GGA+U result, which overestimates the volume.

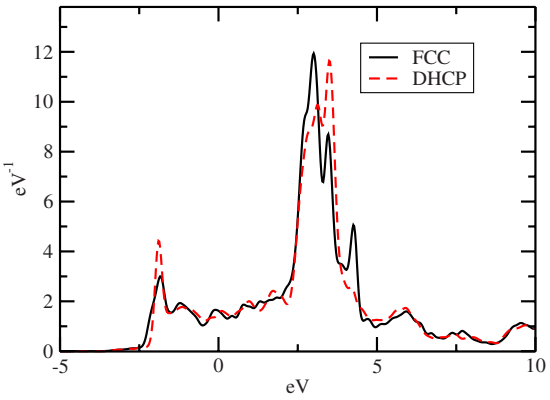

FIG. 4. (Color online) Density of states of γ and β cerium. A smearing of 0.14 eV is used.

As emphasized by Shick *et al.*,[12] metastable states appear in γ cerium. Different energies can be obtained according to the starting point of the calculation. It can be simply explained: During the self-consistent search for the global minimum, it happens that the system is trapped in a local one, with a given repartition of the electrons in the orbitals. So, going to another minimum would require a drastic change in the f wave functions. This is peculiar to methods that create an orbital order and fill only some particular orbitals with electrons. This effect is more important if the symmetry is not imposed during the calculation. Each of these metastable states is, however, associated with a given matrix of occupation. As we do not include the spin-orbit coupling, we can express the occupation matrix in the basis of the real spherical harmonics defined by $S^{m\pm}=(-1)^m\sqrt{2}/(1+i\pm(1-i))(Y_{|m|}\pm Y^*_{|m|})$.[63] In the following, $f^{i\pm}$ is the notation for an f orbital with an angular part $S^{i\pm}$. In

TABLE VI. Cell parameters and volume per atom of β cerium and γ cerium according to experimental data and calculations. For the AFM dhcp structure, three cell parameters are needed (see Fig. 3). Note that LDA and GGA calculations do not give any moment at the theoretical lattice parameter. For the LDA+U calculation, the relaxation is done for the most stable state, which is AFM. The last column gives the energy difference between the antiferromagnetic structure of cerium and the ferromagnetic structure in LDA+U, LDA, and GGA. Calculations of energy are done at the experimental structural parameters, and energy differences are relative to the eight atom unit cell (see Fig. 3).

	dhcp				fcc
	a (Å)	c (Å)	V (Å^3)	$E_{\mathrm{AFM}}-E_{\mathrm{FM}}$ meV	V (Å^3)
Expt.[a]	3.67	11.75	34.22	<0	34.4
LDA (FM)	3.2	10.6	23.2	17	23.2
GGA (FM)	3.4	11.1	27.0	70	26.6
LDA+U (AFM)	7.13/3.63	11.5	32.0	−40	32.1

[a]Reference 54.

the fcc structure, the site symmetry of an atom is cubic and the point group is O_h. Character tables show that the f orbitals split in T_{1u}, T_{2u}, and A_{2u}. We find that, as intuitively expected, putting the f electron inside the f^{2-}, which belongs to the A_{2u} irreducible representation, gives the lowest energy.[64]

2. β cerium

The β phase has a dhcp structure. Due to the hysteresis[1] in the transitions involving γ and α cerium, it is a challenge to determine its structure. Wilkinson *et al.*[65] performed neutron diffraction studies and proposed an antiferromagnetic structure for this phase.[65] However, their structure is nevertheless not consistent because sites with the same magnetization are not equivalent. It has, in fact, been contested by Gibbons *et al.*[54] in a study on alloys of cerium and yttrium. They proposed another antiferromagnetic order, which is presented in Fig. 3.

Even if cerium has only one f electron, the search for the ground state is an involved task because of the number of metastable states in the LDA+U description of β cerium. This is due to the large number of atoms and also to the existence of sites of different local symmetries, namely, cubic and hexagonal (see Fig. 3). In order to find the most stable solution, we carried out different calculations, with several hints for the occupation matrix. We found the lowest ground state with the condition that the system is an antiferromagnet. Starting from the occupation matrix, we computed the ferromagnetic ground state defined by the same occupation matrix. It appears that it leads to the lowest state with this magnetic order. We checked, however, that this state is lower in energy compared to the state extrapolated from the occupation matrix from cubic (fcc) and hexagonal (hcp) crystals (see the Appendix).

In Fig. 4, we present the density of states for both the γ and the β phases of cerium. The spectrum for the γ phase is in good agreement with that found in the work of Shick *et al.*,[28] with peaks located at −2.5 and 3 eV. The position of these peaks is in good agreement with the experimental photoemission spectra,[66,67] even if obtaining a correct width would require going beyond LDA+U.[19,24] The β cerium density of states looks very similar to the γ cerium one. We carried out the calculation for several different metastable states, and we saw only slight modifications in the width of Hubbard bands. All calculations show that the peaks are located at the same place as for γ cerium. This spectrum and the position of the peaks drastically differ from the spectrum obtained from GGA calculation,[32] which does not take into account the strong correlations.

From the experimental phase diagram and from a thermodynamical point of view, one knows that at the transition, the volume of the γ phase is slightly lower than the volume of the β phase. As these two phases are compact, we also expect their volumes to be close. Indeed, the equilibrium volume of β cerium computed in LDA+U is 32.0 Å^3 and is very similar to the volume of γ cerium (32.1 Å^3). Moreover, the total magnetization per atom computed in the ferromagnetic structure is the same as that for γ cerium ($1.1\mu_B$). The magnetic moments computed inside PAW augmentation regions are very similar in the AFM and FM ground states.[68] It confirms the localization of the f electron. However, as LDA+U imposes a magnetic order to γ cerium, we cannot precisely compute the change in volume between the two phases. In fact, the relative difference in volume between different orbital orders of β cerium computed in LDA+U (0.5%) is comparable to the relative difference in volume between the two phases. So, a more correct description of magnetism and its origin is necessary to compute this difference in volume. LDA+DMFT, which takes into account the dynamical fluctuations, is, in fact, able to describe both magnetically ordered and paramagnetic states. The disordered local moment method has also shown some success in the description of the magnetism of heavy lanthanides.[69] As expected, LDA and GGA calculations strongly underestimate the volume by 33% and 22%, respectively, which is similar to what is observed for γ cerium (see Table VI).

As it is a ground-state property, the relative stability of AFM and FM configurations is an important point to be dis-

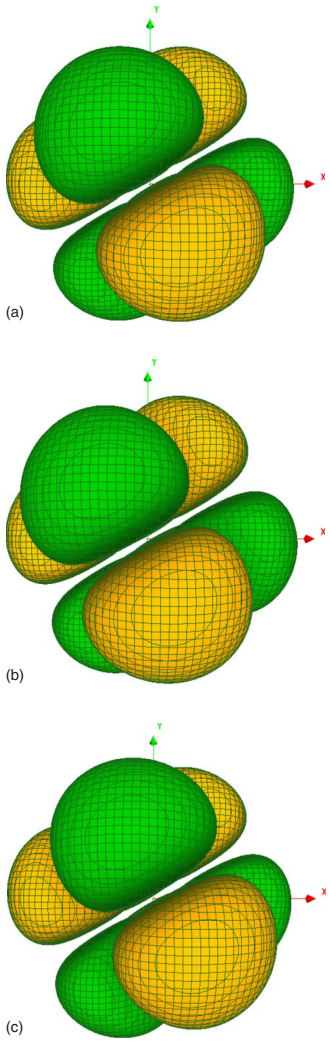

FIG. 5. (Color online) Isodensity curves for the filled orbitals for hexagonal sites [(a) one of the positive lobe is directed along x] and cubic sites [orbitals are slightly tilted with respect to hexagonal sites. (b) Atoms 1 and 2; (c) atoms 3 and 4]. Cartesian axes are the same as in Fig. 3. Two colors are used for the negative and positive values of the isodensity plot.

cussed. We have computed this energy difference by using the LDA+U method and both LDA and GGA methods. The results are given in Table VI and show that LDA+U favors the AFM order with respect to the FM. Note that in the GGA or the LDA approximations, the FM one is the most stable. We checked that this statement is correct for the three lowest metastable states that we have found (see the Appendix). In these three cases, the difference in energy in LDA+U ranges from −40 to −108 meV. So, we can expect that a hypothetical lower ground state—not captured by our calculation—will reproduce this energetic order.

Note that this stabilization is insensitive to the choice of the LDA+U functional: The same result is found with the full localized limit method using $J=0.95$ eV and $U=6.1$ eV. It suggests that this stabilization is due to the interaction of f electrons with s, p, and d electrons depending on the position of f orbitals—as proposed for calculations on gadolinium.[28–30] We checked that the results are still valid when both FM and AFM solutions are relaxed to their lattice equilibrium values. In this case, $E_{\mathrm{AFM}}-E_{\mathrm{FM}}=-44$ meV. In order to compare to gadolinium in a similar situation, we computed the difference in energy between AFM and FM ground states for the hypothetical hcp structure of cerium. We find that the AFM ground state is lower (−17 meV/atom). It shows that the stability of the AFM order is intrinsically due to the element and not to the structure (hcp or dhcp). Note that a study[69] of gadolinium and other heavy lanthanides shows how the stability of ferromagnetism—with respect to incommensurate ordering—is linked to the values of the structural parameters (for a given structure). In this study, however, we focus on the experimental commensurate ordering.

The energy difference between the FM and AFM configurations for β cerium is 5 meV/atom, which is smaller than the value of 20 meV/atom that is found for gadolinium. The temperature of the transition[54] is 7 K for β cerium, whereas it is 293 K for gadolinium. This difference is expected—even if a direct link between the difference in energy and the Curie or the Néel temperature is not straightforward[29]—especially in different structures.

IV. CONCLUSION

We present a study of the β and γ phases of cerium. We reproduce a previous result, where the γ phase is correctly described within the LDA+U framework. We show that the β phase is also correlated, as anticipated from its volume and its magnetic properties. The volumes of the γ and β phases are found to be close because structures are compact. The main result is that the electrons are localized in the β phase and that the antiferromagnetic order is correctly stabilized with respect to the ferromagnetic configuration. We explain some details of our implementation of LDA+U and thoroughly test the method on well known systems. We detail the procedure that we followed to enforce the convergence of self-consistence loop and to find the ground state of this complex phase in terms of occupation matrix for different magnetic orders.

ACKNOWLEDGMENT

We would like to thank Gérald Jomard for useful discussions.

APPENDIX: OCCUPATION MATRIX FOR β CERIUM

In order to check the validity of the state found for the lowest energy, we compared its energy to the solution in which the sites adopt the occupation matrix of the fcc or the hexagonal structure. This solution would be the most stable if f orbitals were completely localized without any interaction, i.e., even through s, p, and d orbitals.

In order to find this solution, we performed calculations for the hcp structure (*ABABAB*, where *A* and *B* are compact planes), where there are only hexagonal sites, and for the fcc structure (*ABCABCABC*), where there are only cubic sites. In the hcp structure, the site symmetry of the cerium atom is hexagonal. In this case, the f level splits into five irreducible representations, namely, B_{1u}, E_{2u}, A_{2u}, E_{1u}, and B_{2u}. We found that the minimum in energy is obtained when the occupation matrix contains only one electron located in the f^0 orbital (which belongs to A_{2u}). In the case of the cubic symmetry, the electron is located inside the f^{2-} orbital, whose angular part is S^{2-}.

The dhcp structure corresponds to a compact structure with an *ABACABAC* stacking. The atoms in the *A* layer have a local cubic environment, whereas the atoms in *B* and *C* layers have a hexagonal environment. Note that for cubic states, a rotation matrix has to be applied to the occupation matrix: For the fcc structure, the f electron in LDA+U is located in the orbital $f^{2-}=\sqrt{105/4\pi}xyz$. In this case, the *ABC* layers are oriented along the (111) direction. In the dhcp structure, the same axis for the cubic sites is oriented along the (100) direction. So, we just had to do a rotation of the f orbitals in order to find a different occupation matrix. We found that the orbitals are transformed into $\sqrt{4/9}f^{3-}+\sqrt{5/9}f^0$ for sites 1 and 3 and into $\sqrt{4/9}f^{3-}-\sqrt{5/9}f^0$ for sites 2 and 4. These orbitals are the eigenvectors in an ideal cubic symmetry. We then have the following for the rotated occupation matrix on the basis of f^{3-} and f^0:

$$\begin{pmatrix} \frac{4}{9}n & \pm\frac{\sqrt{20}}{9}n \\ \pm\frac{\sqrt{20}}{9}n & \frac{5}{9}n \end{pmatrix},$$

where n is the occupation of f^{2-} orbitals in the fcc structure.

We performed self-consistent calculations starting from this occupation matrix and found that the solution is 43 mhartree higher in energy than the ground state. It suggests that our solution is one of the most stable ones.

In our lowest energy solution, the f electron is located—for the cubic sites—in an orbital that is a linear combination of f^{2-}, f^{1-}, f^{1+}, f^{2+}, and f^{3+}. For the hexagonal sites, we found that the f electron is in the orbital $0.60f^{3+}+0.40f^{1+}-0.69253f^{1-}$. These two orbitals for the cubic and hexagonal sites look like f^{2-} orbitals: Their positive lobes are oriented

along the directions of the corners of a tetrahedron. One of the nodal planes of these orbitals is orthogonal to the vector $\vec{j}$ (see Fig. 3). These orbitals are plotted in Fig. 5.

Note, however, that we do not expect the physical properties to drastically change for different states. For example, the variation between the volumes computed in the lowest ground state and in the state whose matrix of occupations is given above is within the precision given in Table VI. The previous description could be easily generalized in the case of spin-orbit coupling.

[1] D. G. Koskimaki and K. A. Gschneidner, *Handbook on the Physics and Chemistry of Rare Earths* (North-Holland, Amsterdam, 1978).
[2] B. Johansson, Philos. Mag. **30**, 469 (1974).
[3] L. de' Medici, A. Georges, G. Kotliar, and S. Biermann, Phys. Rev. Lett. **95**, 066402 (2005).
[4] P. Hohenberg and W. Kohn, Phys. Rev. **136**, B864 (1964).
[5] W. Kohn and L. J. Sham, Phys. Rev. **140**, A1133 (1965).
[6] V. I. Anisimov, J. Zaanen, and O. K. Andersen, Phys. Rev. B **44**, 943 (1991).
[7] V. I. Anisimov, F. Aryasetiawan, and A. I. Lichtenstein, J. Phys.: Condens. Matter **9**, 767 (1997).
[8] A. I. Liechtenstein, V. I. Anisimov, and J. Zaanen, Phys. Rev. B **52**, R5467 (1995).
[9] M. T. Czyżyk and G. A. Sawatzky, Phys. Rev. B **49**, 14211 (1994).
[10] S. Y. Savrasov and G. Kotliar, Phys. Rev. Lett. **84**, 3670 (2000).
[11] J. Bouchet, B. Siberchicot, F. Jollet, and A. Pasturel, J. Phys.: Condens. Matter **12**, 1723 (2000).
[12] A. B. Shick, W. E. Pickett, and A. I. Liechtenstein, J. Electron Spectrosc. Relat. Phenom. **114-116**, 753 (2001).
[13] A. B. Shick, V. Drchal, and L. Havela, Europhys. Lett. **69**, 588 (2005).
[14] A. Georges, G. Kotliar, W. Krauth, and M. J. Rozenberg, Rev. Mod. Phys. **68**, 13 (1996).
[15] V. I. Anisimov, A. I. Poteryaev, M. A. Korotin, A. O. Anokhin, and G. Kotliar, J. Phys.: Condens. Matter **9**, 7359 (1997).
[16] A. I. Lichtenstein and M. I. Katsnelson, Phys. Rev. B **57**, 6884 (1998).
[17] G. Kotliar, S. Y. Savrasov, K. Haule, V. S. Oudovenko, O. Parcollet, and C. A. Marianetti, Rev. Mod. Phys. **78**, 865 (2006).
[18] J. Laegsgaard and A. Svane, Phys. Rev. B **59**, 3450 (1999).
[19] K. Held, A. K. McMahan, and R. T. Scalettar, Phys. Rev. Lett. **87**, 276404 (2001).
[20] A. K. McMahan, K. Held, and R. T. Scalettar, Phys. Rev. B **67**, 075108 (2003).
[21] A. K. McMahan, Phys. Rev. B **72**, 115125 (2005).
[22] K. Haule, V. Oudovenko, S. Y. Savrasov, and G. Kotliar, Phys. Rev. Lett. **94**, 036401 (2005).
[23] O. Sakai, Y. Shimizu, and Y. Kaneta, J. Phys. Soc. Jpn. **74**, 2517 (2005).
[24] B. Amadon, S. Biermann, A. Georges, and F. Aryasetiawan, Phys. Rev. Lett. **96**, 066402 (2006).
[25] G. Sangiovanni *et al.*, Phys. Rev. B **73**, 205121 (2006).
[26] A. Svane, Phys. Rev. B **53**, 4275 (1996).
[27] M. Lüders, A. Ernst, M. Däne, Z. Szotek, A. Svane, D. Ködderitzsch, W. Hergert, B. L. Györffy, and W. M. Temmerman, Phys. Rev. B **71**, 205109 (2005).
[28] A. B. Shick, A. I. Liechtenstein, and W. E. Pickett, Phys. Rev. B **60**, 10763 (1999).
[29] Ph. Kurz, G. Bihlmayer, and S. Blügel, J. Phys.: Condens. Matter **14**, 6353 (2002).
[30] M. Petersen, J. Hafner, and M. Marsman, J. Phys.: Condens. Matter **18**, 7021 (2006).
[31] R. S. Rao, C. K. Majumdar, and R. P. Singh, Phys. Rev. B **19**, 6274 (1979).
[32] K. T. Moore, B. W. Chung, S. A. Morton, A. J. Schwartz, J. G. Tobin, S. Lazar, F. D. Tichelaar, H. W. Zandbergen, P. Söderlind, and G. van der Laan, Phys. Rev. B **69**, 193104 (2004).
[33] X. Gonze, J.-M. Beuken, R. Caracas, F. Detraux, M. Fuchs, G.-M. Rignanese, L. Sindic, M. Verstraete, G. Zerah, F. Jollet, M. Torrent, A. Roy, M. Mikami, Ph. Ghosez, J.-Y. Raty, and D. C. Allan, Comput. Mater. Sci. **25**, 478 (2002).
[34] X. Gonze *et al.*, Z. Kristallogr. **220**, 558 (2005).
[35] The ABINIT code is a common project of the Université Catholique de Louvain, Corning Incorporated, the Université de Liège, the Commissariat à l'Energie Atomique, Mitsubishi Chemical Corp., the Ecole Polytechnique Palaiseau, and other contributors (http://www.abinit.org).
[36] For *d* orbitals, we used $F_4/F_2=0.625$, and for *f* orbitals, we used $F_4/F_2=0.6681$ and $F_6/F_2=0.4943$.
[37] S. L. Dudarev, G. A. Botton, S. Y. Savrasov, C. J. Humphreys, and A. P. Sutton, Phys. Rev. B **57**, 1505 (1998).
[38] P. E. Blöchl, Phys. Rev. B **50**, 17953 (1994).
[39] O. Bengone, M. Alouani, P. Blöchl, and J. Hugel, Phys. Rev. B **62**, 16392 (2000).
[40] G. Kresse and D. Joubert, Phys. Rev. B **59**, 1758 (1999).
[41] M. Torrent, F. Jollet, F. Bottin, G. Zerah, and X. Gonze, Comput. Mater. Sci. **42**, 337 (2008).
[42] A. K. Cheetham and D. A. O. Hope, Phys. Rev. B **27**, 6964 (1983).
[43] H. A. Alperin, J. Phys. Soc. Jpn. **17**, 12 (1962).
[44] W. Neubeck, C. Vettier, V. Fernandez, F. de Bergevin, and C. Giles, J. Appl. Phys. **85**, 4847 (1999).
[45] G. A. Sawatzky and J. W. Allen, Phys. Rev. Lett. **53**, 2339 (1984).
[46] S. Hüfner, J. Osterwalder, T. Riesterer, and F. Hulliger, Solid State Commun. **52**, 793 (1984).
[47] S. L. Dudarev, A. I. Liechtenstein, M. R. Castell, G. A. D. Briggs, and A. P. Sutton, Phys. Rev. B **56**, 4900 (1997).
[48] O. Eriksson, R. Ahuja, A. Ormeci, J. Trygg, O. Hjortstam, P. Söderlind, B. Johansson, and J. M. Wills, Phys. Rev. B **52**, 4420 (1995).
[49] I. Turek, J. Kudrnovský, G. Bihlmayer, and S. Blügel, J. Phys.: Condens. Matter **15**, 2771 (2003).
[50] A. R. Tackett, N. A. W. Holzwarth, and G. E. Matthews, Comput. Phys. Commun. **135**, 348 (2001).
[51] N. A. W. Holzwarth, M. Torrent, and F. Jollet, ATOMPAW (http://pwpaw.wfu.edu/) and ATOMPAW2ABINIT (http://www.abinit.org).
[52] D. Vanderbilt, Phys. Rev. B **41**, 7892 (1990).

[53] V. I. Anisimov and O. Gunnarsson, Phys. Rev. B **43**, 7570 (1991).
[54] E. P. Gibbons, E. M. Forgan, and K. A. McEwen, J. Phys. F: Met. Phys. **17**, L101 (1987).
[55] P. Söderlind, O. Eriksson, B. Johansson, and J. M. Wills, Phys. Rev. B **50**, 7291 (1994).
[56] P. Ravindran, L. Nordström, R. Ahuja, J. M. Wills, B. Johansson, and O. Eriksson, Phys. Rev. B **57**, 2091 (1998).
[57] I.-K. Jeong, T. W. Darling, M. J. Graf, Th. Proffen, R. H. Heffner, Y. Lee, T. Vogt, and J. D. Jorgensen, Phys. Rev. Lett. **92**, 105702 (2004).
[58] J. S. Olsen, L. Gerward, U. Benedict, and J.-P. Itié, Physica B & C **133**, 129 (1985).
[59] L. V. Pourovskii, B. Amadon, S. Biermann, and A. Georges, Phys. Rev. B **76**, 235101 (2007).
[60] B. Johansson, I. A. Abrikosov, M. Aldén, A. V. Ruban, and H. L. Skriver, Phys. Rev. Lett. **74**, 2335 (1995).
[61] F. Aryasetiawan, K. Karlsson, O. Jepsen, and U. Schönberger, Phys. Rev. B **74**, 125106 (2006).
[62] M. E. Manley, R. J. McQueeney, B. Fultz, R. Osborn, G. H. Kwei, and P. D. Bogdanoff, Phys. Rev. B **65**, 144111 (2002).
[63] M. A. Blanco, M. Flórez, and M. Bermejo, J. Mol. Struct.: THEOCHEM **419**, 19 (1997).
[64] Slightly lower solutions in energy can also be obtained by artificially breaking the cubic symmetry. Nevertheless, our result is consistent with the results found by Shick *et al.* (Ref. 12). However, to precisely reproduce them, one should include spin-orbit coupling in the calculation.
[65] M. K. Wilkinson, H. R. Child, C. J. McHargue, W. C. Koehler, and E. O. Wollan, Phys. Rev. **122**, 1409 (1961).
[66] E. Wuilloud, H. R. Moser, W.-D. Schneider, and Y. Baer, Phys. Rev. B **28**, 7354 (1983).
[67] D. Wieliczka, J. H. Weaver, D. W. Lynch, and C. G. Olson, Phys. Rev. B **26**, 7056 (1982).
[68] The use of spin-orbit coupling and nonlinear magnetism would permit us to have a more precise value for the magnetic moment; however, we do not expect that the physical picture describing the localization of one *f* electron would change.
[69] I. D. Hughes, M. Däne, A. Ernst, W. Hergert, M. Lüders, J. Poulter, J. B. Staunton, A. Svane, Z. Szotek, and W. M. Temmerman, Nature (London) **446**, 650 (2007).